

Noncoherent Hybrid Parallel PN Code Acquisition for CDMA Mobile Communications

Wei-hua Zhuang, *Member, IEEE*

Abstract—This paper proposes a noncoherent hybrid parallel pseudonoise (PN) code acquisition scheme for code-division multiple access (CDMA) mobile communication systems and analyzes the effect of multiple access interference (MAI) on the code acquisition performance for Rayleigh and Rician fading channels. The hybrid acquisition scheme combines parallel search with serial search to cover the whole uncertainty region of the input code phase. It has a much simpler acquisition hardware structure than the total parallel acquisition and can achieve the mean acquisition time slightly inferior to that of the total parallel acquisition in the case of severe MAI; on the other hand, it provides the flexibility in the tradeoff between the mean acquisition time and system complexity if no MAI is considered. The closed-form expressions of the detection and false-alarm probabilities and mean acquisition time are derived. Numerical analysis quantifies the severe performance degradation of code acquisition due to both MAI and channel fading, and demonstrates the dependence of the increase of mean acquisition time (due to MAI) on the number of users in the CDMA system, system design parameters, and channel fading statistics.

I. INTRODUCTION

RECENTLY, there has been considerable interest in the application of direct-sequence spread-spectrum (DS/SS) multiple access, also known as code-division multiple access (CDMA), to cellular and personal communication systems [1]–[4]. CDMA has significant advantages in the areas of capacity, frequency planning, continuous call quality, privacy, and resistance to multipath fading. Pseudonoise (PN) code synchronizer is an essential element of CDMA mobile communication systems because data transmission is possible only after the spread spectrum receiver accurately synchronizes the locally generated PN code with the incoming PN code. The code synchronization is usually achieved in two steps, i.e., acquisition and tracking. Code acquisition is to achieve coarse alignment within some fraction of one code-chip interval between the two PN codes, and the tracking process is to achieve fine alignment between the PN codes, which further reduces synchronization error to an allowed limit. In a CDMA environment, code acquisition specifically refers to the task of obtaining a PN code phase estimate of the intended data transmission. The code acquisition is subject to mobile channel fading; furthermore, the acquisition has to be achieved in the

presence of multiple access interference (MAI) due to other users in the same cell and surrounding cells, since many users share the same radio spectrum by using different PN codes. In the design of the acquisition system, an important performance measure is the average of the time that elapses prior to acquisition, T_{acq} , and another major concern is the synchronizer hardware complexity.

Various techniques have been proposed for rapid code acquisition, which can be classified as either serial search or parallel search. Serial search steps through the uncertainty region of the incoming code phase sequentially. Polydoros and Weber [5] have proposed a rapid noncoherent I - Q detector for serial search in an additive white Gaussian noise (AWGN) channel, which enables decisions to be made on the order of the DS code chip duration, thereby significantly reducing the acquisition time. On the other hand, parallel search uses a bank of matched filters, each matched to a different waveform pattern of PN code subsequences corresponding to all possible PN code phases, and then make a decision based on all the outputs of the filters. Milstein *et al.* [6] have proposed and analyzed parallel acquisition to reduce acquisition time for DS/SS communications in an AWGN channel. Sourour and Gupta [7], [8] have extended the analysis on parallel acquisition to fading channels. Recently, Madhow and Pursley [9] have studied the effect of MAI on code acquisition with coherent detection, and Rick and Milstein [10] with noncoherent detection, however for an AWGN channel only. The effect of MAI on PN code acquisition performance has not been analyzed theoretically for mobile fading channels in open literature.

In CDMA systems, whether parallel search or serial search should be used for code acquisition depends on system design criteria. The totally parallel acquisition scheme simultaneously tests all possible code phases, therefore, can significantly reduce the code acquisition time. The hardware complexity, however, increases dramatically. The number of parallel noncoherent matched filters is equal to that of all possible (discrete) PN code phases, which can be a very large number for a long PN code sequence. On the other hand, a serial search technique can achieve receiver hardware simplicity at the expense of code acquisition speed. The tradeoff between totally parallel search and serial search is the acquisition time versus system hardware cost. In this paper, a noncoherent hybrid parallel acquisition scheme which combines parallel search with serial search is proposed for code acquisition in the presence of MAI over fading channels. The scheme can achieve a balance between the acquisition speed and system

Manuscript received November 12, 1994; revised March 11, 1995. This work was presented in part at the 1995 International Conference on Wireless Communications, Calgary, July 10–12, 1995. This work was supported by research grants by NSERC (the Natural Sciences and Engineering Research Council of Canada) and ITRC (the Information Technology Research Center—Center of Excellence supported by Technology Ontario).

The author is with the Department of Electrical and Computer Engineering, University of Waterloo, Waterloo, ON, N2L 3G1 Canada.

Publisher Item Identifier S 0018-9545(96)08204-7.

complexity. The effect of MAI on the acquisition performance is analyzed theoretically for Rayleigh and Rician fading channels. A more realistic mobile fading channel model is used here as compared with that used in [7] and [8]. Previously, channel fading process was assumed to be time-invariant over several successive chips. In this paper, a continuously time-varying channel fading process is considered.

The paper is organized as follows. Section II analyzes the effect of MAI on the performance of noncoherent correlators for code acquisition in mobile fading channels. Section III studies the hybrid parallel acquisition scheme, where parallel search is combined with serial search to cover the whole uncertainty region of the input code phase. The closed-form expressions of the detection and false-alarm probabilities and mean acquisition time are derived. The code acquisition performance in the presence of MAI over mobile fading channels is evaluated in Section IV based on numerical analysis. The conclusions of this work are presented in Section V.

II. EFFECT OF MULTIPLE ACCESS INTERFERENCE IN FADING CHANNELS

In a binary phase shift keying (BPSK) CDMA communication system, the transmitted signal of the target transmission link can be represented as

$$s(t) = \sqrt{2P}c_1(t + \xi'_1 T_c) \cos(\omega t + \theta'_1) \quad (1)$$

where P is the signal power, $c_1(t) \triangleq \sum_{i=-\infty}^{\infty} c_{1,i} p_{T_c}(t - iT_c)$, $c_{1,i} \in \{-1, +1\}$ is the i th element of the PN code sequence, $p_{T_c}(t)$ is the PN code waveform defined as a unit rectangular pulse over $[0, T_c]$, ξ'_1 is the PN code phase normalized to the chip interval T_c , ω is the carrier radian frequency, and θ'_1 is the carrier phase at $t = 0$. Without *a priori* information of input code phase, the uncertainty region of the code phase is the full code period Θ . If a special preamble or a pilot signal is used for the purpose of acquisition, then the code acquisition starts and ends before the data stream is introduced; therefore, the effect of data modulation is not considered here for code acquisition.

The transmitted signal reaches the receiver via one or more propagation paths. The received signal consists of a deterministic line-of-sight (LOS) component (if it exists) and other reflected and scattered multipath components. A frequency non-selective multipath fading channel introduces a time-variant amplitude fluctuation, carrier phase jitter, and propagation delay to the signaling waveform transmitted through it. The complex impulse response of a Rician fading channel at baseband can be represented as

$$h(t) = \{\gamma \exp(j\phi) + \alpha(t) \exp[j\varphi(t)]\} \delta(t - \tau) \quad (2)$$

where $\gamma \exp(j\phi)$ represents the deterministic component due to the existing LOS path between the transmitter and receiver, $\alpha(t) \exp[j\varphi(t)]$ represents the diffusive component due to multipath propagation, τ is the propagation delay, and $\delta(\cdot)$ is the Dirac delta function. Generally, $\alpha(t)$ is Rayleigh distributed, and $\varphi(t)$ is uniformly distributed over $[0, 2\pi]$. The diffusive component can also be represented as a complex Gaussian random process, $\alpha(t) \exp[j\varphi(t)] = x(t) + jy(t)$,

with $x(t)$ and $y(t)$ being independent Gaussian random processes with zero mean and variance σ_f^2 . The ratio of the average power of the deterministic signal component to that of the diffusive signal component is defined as k -factor, i.e., $k \triangleq \gamma^2 / 2\sigma_f^2$. When the k factor approaches ∞ dB, the diffusive component due to multipath at the received signal disappears and the fading channel becomes an AWGN channel. On the other hand, when the k factor approaches to $-\infty$ dB, the LOS deterministic component vanishes and the channel becomes Rayleigh fading channel.

Considering the case that the system has L users, each of the L transmitted signals arriving at the receiver with independent random carrier phases ϕ_i and θ_i uniformly distributed over $[0, 2\pi]$ and an independent random propagation delay τ_i , $i = 1, 2, \dots, L$ (where $i = 1$ represents the target transmission), the received signal can be represented as

$$\begin{aligned} r(t) = & \sqrt{2P} \sum_{i=1}^L \gamma_i c_i(t + \xi_i T_c) \cos(\omega t + \theta_i + \phi_i) \\ & + \sqrt{2P} \sum_{i=1}^L x_i(t) c_i(t + \xi_i T_c) \cos(\omega t + \theta_i) \\ & + \sqrt{2P} \sum_{i=1}^L y_i(t) c_i(t + \xi_i T_c) \\ & \cdot \sin(\omega t + \theta_i) + n(t) \end{aligned} \quad (3)$$

where $\xi_1 = \xi'_1 - \tau/T_c$ (i.e., $i = 1$) is the code phase delay of the desired signal of the target transmission normalized to the chip duration T_c , $c_i(t + \xi_i T_c)$ is the PN code waveform of the MAI signal from the i th user in the system with a normalized code phase delay ξ_i ($i = 2, 3, \dots, L$), $\theta'_i = \theta_i + \omega\tau$, and $n(t) = n_c(t) \cos(\omega t) + n_s(t) \sin(\omega t)$ with $n_c(t)$ and $n_s(t)$ having zero-mean and one-sided power spectral density N_0 and being mutually independent Gaussian random processes at baseband. Without losing the generality, we take the carrier phase of the desired signal as a reference, i.e., $\theta_1 = 0$, since the effect of θ_1 can be combined with that of the phase shift ϕ_1 in the direct path and that of φ_1 in the multipath propagation. In the following analysis, it is assumed that: for any given PN sequence $\{c_{j,i}\}$ ($j = 1, 2, \dots, L$) with a very long period, the elements $c_{j,i}$ are independent and identically distributed, taking the values $+1$ and -1 with equal probability. As a result, the partial autocorrelation function of the PN codes is approximated by the full autocorrelation function of the PN codes.

At the receiver, a partial correlation of the incoming and locally generated codes is performed at baseband in the in-phase and quadrature arms, squared in each arm and added as a decision variable e_{ij} for the j th branch over the i th interval of duration $T \triangleq MT_c$, as shown in Fig. 1, where Δ is a design parameter to be described in Section III. The receiver generates local in-phase (I) and quadrature (Q) signals to noncoherently correlate the input PN code signal of the target transmission

$$\begin{bmatrix} I(t) \\ Q(t) \end{bmatrix} = \begin{bmatrix} 2c_1(t + \hat{\xi}_1 T_c) \cos(\omega t) \\ 2c_1(t + \hat{\xi}_1 T_c) \sin(\omega t) \end{bmatrix} \quad (4)$$

where $\hat{\xi}_1$ is the normalized code phase offset of the receiver locally generated subcode. The noncoherent correlators perform “integrate and dump” function and output

$$\begin{bmatrix} e_I \\ e_Q \end{bmatrix} = \begin{bmatrix} \frac{1}{T} \int_0^T r(t)I(t) dt \\ \frac{1}{T} \int_0^T r(t)Q(t) dt \end{bmatrix}. \quad (5)$$

Substituting (3) and (4) into (5), it can be derived that

$$e_I = S_{dI} + S_{fI} + D_{dI} + D_{fI} + N_I. \quad (6)$$

The components of e_I in (6) are as follows:

- 1) S_{dI} is the component of the target transmission from the LOS path

$$\begin{aligned} S_{dI} &= \frac{1}{T} \int_0^T \left[\gamma_1 \sqrt{2P} c_1(t + \xi_1 T_c) \cos(\omega t + \phi_1) \right] I(t) dt \\ &= \gamma_1 \sqrt{2P} \cos(\phi_1) R_c(\epsilon_1) \end{aligned} \quad (7)$$

with $\epsilon_1 = |\xi_1 - \hat{\xi}_1|$ being the absolute value of the code phase synchronization error normalized to a chip duration and $R_c(\cdot)$ is the autocorrelation function of the PN code $c_1(t)$

$$\begin{aligned} R_c(\epsilon) &= \frac{1}{T} \int_0^T c_1(t + \xi_1 T_c) c_1(t + \hat{\xi}_1 T_c) dt \\ &= \begin{cases} 1 - \epsilon, & \epsilon < 1 \text{ (“}H_1\text{” state);} \\ 0, & \epsilon \geq 1 \text{ (“}H_0\text{” state).} \end{cases} \end{aligned} \quad (8)$$

- 2) S_{fI} is the diffusive component of the target transmission due to multipath

$$S_{fI} = \frac{1}{T} \int_0^T \sqrt{2P} x_1(t) c_1(t + \xi_1 T_c) c_1(t + \hat{\xi}_1 T_c) dt. \quad (9)$$

Since $x_1(t)$ is a Gaussian random process with zero mean and $c_1(t + \xi_1 T_c) c_1(t + \hat{\xi}_1 T_c)$ is a random process which takes on value of either +1 or -1 equally likely, S_{fI} is a Gaussian random variable with mean $E[S_{fI}] = 0$ and variance σ_{fI}^2 , represented as $S_{fI} \sim G(0, \sigma_{fI}^2)$, where

$$\begin{aligned} \sigma_{fI}^2 &= \frac{2P}{T^2} \int_0^T \int_0^T E[x_1(t)x_1(s)] E[c_1(t + \xi_1 T_c) \\ &\quad \cdot c_1(s + \xi_1 T_c) c_1(t + \hat{\xi}_1 T_c) c_1(s + \hat{\xi}_1 T_c)] ds dt \\ &= \frac{4P}{T^2} \int_0^T (T - \rho) R_{x1}(\rho) F(\rho, \epsilon_1) d\rho \end{aligned} \quad (10)$$

with $\rho \triangleq t - s$, $R_{x1}(\rho) = E[x_1(t)x_1(t - \rho)]$ being the autocorrelation function of the channel fading process $x_1(t)$ and

$$F(\rho, \epsilon) \triangleq E[c_1(t)c_1(t - \rho)c_1(t + \epsilon T_c)c_1(t - \rho + \epsilon T_c)]. \quad (11)$$

For $M \gg 1$ and $\epsilon \geq 0$, $F(\rho, \epsilon)$ can be derived as [11]

$$F(\rho, \epsilon) = \begin{cases} (1 - 2\epsilon) + \epsilon \sum_{n=-\infty}^{\infty} \Lambda(\rho - nT_c, \epsilon T_c) \\ \quad + \epsilon \sum_{m=-\infty}^{\infty} \Lambda(\rho - m\Theta T_c, \epsilon T_c) \\ \quad \text{if } 0 \leq \epsilon \leq \frac{1}{2} \\ (1 - \epsilon) \sum_{n=-\infty}^{\infty} \Lambda(\rho - nT_c, T_c - \epsilon T_c) \\ \quad + \epsilon \sum_{m=-\infty}^{\infty} \Lambda(\rho - m\Theta T_c, \epsilon T_c) \\ \quad \text{if } \frac{1}{2} < \epsilon \leq 1 \\ R_c^2\left(\frac{|\rho|}{T_c}\right) \quad \text{if } \epsilon > 1 \end{cases}$$

where $\Lambda(t, \alpha) \triangleq R_c(|t|/\alpha)$ for $\alpha > 0$.

- 3) D_{dI} is the MAI components from the LOS paths corresponding to all nontarget transmission

$$\begin{aligned} D_{dI} &= \frac{1}{T} \int_0^T \left[\sqrt{2P} \sum_{i=2}^L \gamma_i c_i(t + \xi_i T_c) \right. \\ &\quad \left. \cdot \cos(\omega t + \phi + \theta_i) \right] I(t) dt \\ &= \sqrt{2P} \sum_{i=2}^L \gamma_i y_i \cos(\phi + \theta_i) \end{aligned} \quad (12)$$

where $y_i = (1/T) \int_0^T c_i(t + \xi_i T_c) c_1(t + \hat{\xi}_1 T_c) dt$ is the partial cross-correlation of the PN code sequence $c_i(t + \xi_i T_c)$ of the i th user ($i = 2, 3, \dots, L$) with code phase delay $\xi_i T_c$, and the receiver locally generated PN code sequence $c_1(t + \hat{\xi}_1 T_c)$ for the target transmission. Representing the difference between the two normalized code phase delays as $|\xi_i - \hat{\xi}_1| = \eta_i + \epsilon_i$, where η_i is an integer, and $0 \leq \epsilon_i < 1$, the cross-correlation can be calculated by [11]

$$\begin{aligned} y_i &= \frac{1}{M} \left[(1 - \epsilon_i) \sum_{n=0}^{M-1} c_{1,n} c_{i,n-\eta_i} \right. \\ &\quad \left. + \epsilon_i \sum_{n=0}^{M-1} c_{1,n-1} c_{i,n-\eta_i} \right]. \end{aligned} \quad (13)$$

Since $c_{1,n}$ and $c_{i,n}$ are independent random variables taking on +1 and -1 values with equal probability, based on the Central Limit Theorem [12], y_i has a Gaussian distribution when $M \gg 1$ with mean $E[y_i] = 0$ and variance $\sigma_{y_i}^2 = E[y_i^2] \simeq 2/3M$. Due to the random phase θ_i uniformly distributed over $[0, 2\pi]$, each term in D_{dI} of (12) is independent of any other terms, therefore, D_{dI} is a Gaussian random variable, $D_{dI} \sim G[0, 2P(\sum_{i=2}^L \gamma_i^2)/3M]$.

4) D_{fI} is the MAI resulting from multipath propagation

$$D_{fI} = \frac{1}{T} \int_0^T \sqrt{2P} \left\{ \sum_{i=2}^L [x_i(t)c_i(t + \xi_i T_c) \cos(\omega t + \theta_i)] + \sum_{i=2}^L [y_i(t)c_i(t + \xi_i T_c) \sin(\omega t + \theta_i)] \right\} I(t) dt$$

$$= \sum_{i=2}^L \sqrt{2P} [u_i \cos(\theta_i) + v_i \sin(\theta_i)]. \quad (14)$$

In (14), $u_i = (1/T) \int_0^T x_i(t)c_i(t + \xi_i T_c)c_1(t + \hat{\xi}_1 T_c) dt$ is a Gaussian random variable with mean $E[u_i] = 0$ and variance (see Appendix)

$$\sigma_{u_i}^2 = E[u_i^2]$$

$$= \frac{2}{T^2} \int_0^{T_c} (T - \rho) R_{x_i}(\rho) \left(1 - \frac{\rho}{T_c}\right)^2 d\rho. \quad (15)$$

$v_i = (1/T) \int_0^T y_i(t)c_i(t + \xi_i T_c)c_1(t + \hat{\xi}_1 T_c) dt$ is also a Gaussian random variable with mean $E[v_i] = 0$ and variance the same as that of u_i , provided that $y_i(t)$ has the same autocorrelation function as $x_i(t)$, i.e., $R_{y_i}(\rho) = R_{x_i}(\rho)$. Since $\theta_i (i = 2, 3, \dots, L)$ are independent random variables, each uniformly distributed over $[0, 2\pi]$, it can be shown that D_{fI} is a Gaussian random variable with mean $E[D_{fI}] = 0$ and variance $2P \sum_{i=2}^L \sigma_{u_i}^2$, i.e., $D_{fI} \sim G(0, 2P \sum_{i=2}^L \sigma_{u_i}^2)$.

5) The in-phase component $n_c(t) \cos(\omega t)$ of the input white Gaussian noise $n(t)$ results in the noise component N_I

$$N_I = \frac{1}{T} \int_0^T [n_c(t) \cos(\omega t)][2c_1(t + \hat{\xi}_1 T_c) \cos(\omega t)] dt$$

$$= \frac{1}{T} \int_0^T n_c(t)c_1(t + \hat{\xi}_1 T_c) dt. \quad (16)$$

It can be easily shown that N_I is a Gaussian random variable, $N_I \sim G(0, N_0/2T)$.

In summary, e_I is a Gaussian random variable with mean

$$\mu_I = \sqrt{2P}\gamma_1 \cos(\phi_1)R_c(\epsilon_1) \quad (17)$$

and variance

$$\sigma_I^2 = \frac{2P \sum_{i=2}^L \gamma_i^2}{3M} + 2P \sum_{i=2}^L \sigma_{u_i}^2 + \sigma_{fI}^2 + \frac{N_0}{2T}. \quad (18)$$

In the right-hand side of (18), the first two terms quantify the effect of MAI on the "integrate and dump" filter output of the in-phase arm, the third term characterizes the effect of channel fading, and the last term comes from the input AWGN noise. From (18), we see that the effect of MAI increases as the number of the users in the system increases.

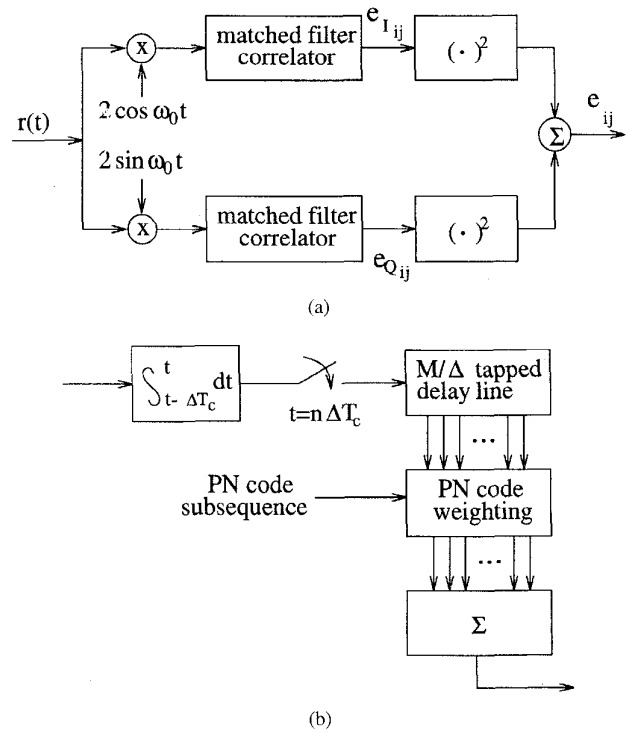


Fig. 1. (a) I - Q noncoherent correlator and (b) structure of the matched filter correlator.

Similarly, it can be derived that e_Q is a Gaussian random variable with mean

$$\mu_Q = \sqrt{2P}\gamma_1 \sin(\phi_1)R_c(\epsilon_1) \quad (19)$$

and variance the same as that of e_I . Note that the variance of e_I and e_Q is a function of the normalized code synchronization error ϵ_1 as can be observed from (10). In the following, we represent the variance of e_I and e_Q as σ_1^2 if the incoming code phase is correctly acquired (i.e., $\epsilon_1 < 1$, representing an " H_1 " state), and σ_0^2 otherwise (i.e., $\epsilon_1 \geq 1$, representing an " H_0 " state).

The decision variable is $e \triangleq e_I^2 + e_Q^2$. It has a noncentral χ^2 distribution at the state " H_1 " with probability density function (pdf)

$$f(e|H_1) = \frac{1}{2\sigma_1^2} \exp\left(-\frac{\nu^2 + e}{2\sigma_1^2}\right) I_0\left(\frac{\nu\sqrt{e}}{\sigma_1^2}\right) \quad (20)$$

where $\nu^2 = \mu_I^2 + \mu_Q^2 = 2P\gamma_1^2 R_c^2(\epsilon_1)$ under the condition of $0 \leq \epsilon_1 < 1$. Equation (20) indicates how the LOS signal component (γ) and code alignment error (ϵ_1) affects the correlator output. When the system is at an " H_0 " state, $\epsilon_1 \geq 1$ and $\nu^2 = 0$, the decision variable e has a central χ^2 distribution with pdf

$$f(e|H_0) = \frac{1}{2\sigma_0^2} \exp\left(-\frac{e}{2\sigma_0^2}\right). \quad (21)$$

The above analysis describes how MAI affects the pdf of the decision variables. With a decrease of γ and/or an increase of ϵ_1 , the difference between the mean values of the decision variable e corresponding to an " H_1 " state and an

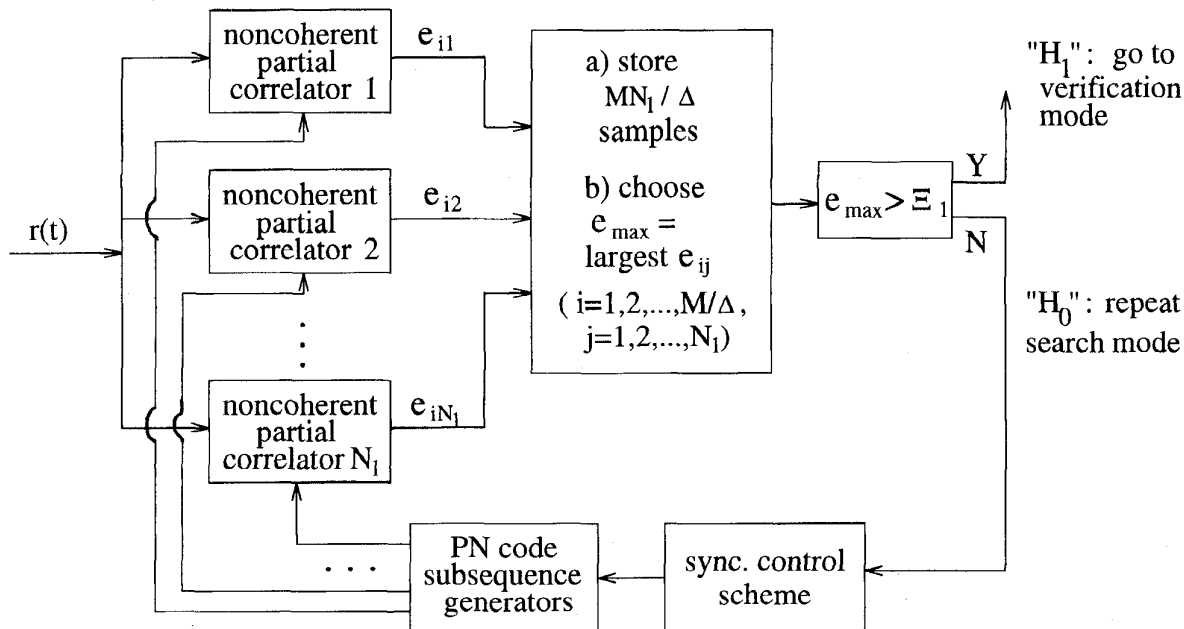


Fig. 2. Noncoherent partial parallel PN code acquisition system.

" H_0 " state is reduced; on the other hand, with an increase of MAI, the variances of both the noncoherent correlator outputs σ_1^2 and σ_0^2 increase proportionally. Both factors reduce the difference between the conditional pdf's $f(e|H_1)$ and $f(e|H_0)$, which can deteriorate code acquisition performance. The effect on MAI on code acquisition performance (such as mean acquisition time) depends on both MAI and code acquisition scheme. In the following, the noncoherent hybrid parallel acquisition is proposed, and the above analysis on the effect of MAI, (20) and (21), will be used in deriving the detection and false alarm probabilities and evaluating the mean acquisition time of the proposed acquisition scheme.

III. HYBRID PARALLEL ACQUISITION

The functional block diagram of the hybrid parallel acquisition system is shown in Fig. 2, which consists of a bank of N_1 parallel noncoherent I - Q correlators, a digital phase alignment detector, and synchronization control logic. The uncertainty region of the input code phase (i.e., the code length, Θ) is divided into sub-regions each having length $M = \Theta / (N_1 \times N_2)$ with N_1 and N_2 being integers. N_1 and N_2 are design parameters describing the numbers of parallel and serial acquisition searches, respectively. For a certain value of Θ , the parameters N_1 and N_2 are inversely proportional to each other. We assume that $\Theta / (N_1 \times N_2)$ is an integer for simplicity. Each correlator has one of the subcodes of length M as a reference code input. The code phase uncertainty region of each subcode is discretized with a step size of Δ , which is normalized to the chip interval T_c . That is, each subcode contains M/Δ discrete PN code phases. Normally $\Delta = 2^{-n}$ with a nonnegative integer n . A typical value of Δ is $1/2$, which is used in the numerical analysis to be discussed. In the partial noncoherent correlation at each correlator, the number of taps on the delay line is M/Δ with a

ΔT_c delay between successive taps, as shown in Fig. 1(b). The incoming code phase uncertainty region is searched in discrete steps. Over each noncoherent correlation period, $T (= MT_c)$, there are MT_c/Δ input data samples. Each new input data sample is collected and, together with previous $MT_c/\Delta - 1$ input samples, is correlated with the N_1 subcodes loaded in the N_1 parallel correlators simultaneously. The process repeats M/Δ times, each time with a unique code phase offset between the incoming PN code and the subcode loaded in any correlator, until all the possible PN code phases corresponding to the N_1 subcodes are tested once. The correlators generate MN_1/Δ decision variables over the period, corresponding to the MN_1/Δ possible phases, respectively. In the next period of duration T , the N_1 noncoherent correlators are loaded with a new group of PN subcodes corresponding to another MN_1/Δ possible input code phases, and the correlation process continues until a coarse code phase alignment is sensed. In this way, over a period of N_2T , the N_1 parallel noncoherent correlators generate Θ/Δ decision variables corresponding to all possible discrete PN code phases of the input signal. The time duration $T - \Delta$ for collecting the initial $MT_c/\Delta - 1$ input signal samples is negligible when compared with the mean acquisition time.

The above hybrid parallel acquisition scheme combines parallel acquisition with serial acquisition. The parameters N_1 and N_2 can be selected to achieve a balance between the acquisition speed and system complexity. The unique aspect of the acquisition scheme is the introduction of the serial search (characterized by the parameter N_2). The parallel acquisition scheme described in [7] and [8] is a special case of the system proposed here with $N_2 = 1$. In the case that the PN code has a very long period (i.e., a large Θ value), both M and N_1 can be very large if using completely parallel acquisition scheme (i.e., $N_2 = 1$), corresponding to a high complexity of the synchronizer. If we choose $N_2 > 1$, we can reduce the number

of noncoherent correlators; however, the mean acquisition time may increase consequently. Hence, the choice of parameters N_1 and N_2 depends on the system design criteria, other system parameters (such as Θ and Δ), radio fading channel statistics, and MAI. In the following, the acquisition performance of the hybrid parallel scheme is analyzed theoretically in order to give a quantitative description of the mean acquisition time as a function of N_1 and N_2 , so that the design parameters can be optimized according to system design criteria and channel characteristics.

Double dwell search with search mode and verification mode [5] is used. In the first dwell search, a decision on whether a coarse alignment is achieved is made after the MN_1/Δ discrete code phases (of the N_1 subcodes loaded in the N_1 parallel branches) are tested once. In other words, after each interval of length T , the decision is made according to the MN_1/Δ decision variables (each corresponding to one of the MN_1/Δ code phases). The decision device stores the MN_1/Δ decision variables and chooses $e_{\max} = \text{largest } e_{ij}$ ($i = 1, 2, \dots, M/\Delta$, and $j = 1, 2, \dots, N_1$). If e_{\max} exceeds the threshold Ξ_1 , the corresponding phase of the subcode is tentatively assumed to be coarsely aligned with the received PN code signal (represented by an " H_1 " state); otherwise, no coarse alignment is achieved (represented by an " H_0 " state), and over next period T , the search process is repeated with the next group of possible reference subcodes until a tentative " H_1 " state is assumed. Then, a verification mode starts. The receiver advances the phase of locally generated PN code at the same rate as the input PN code so that the two codes will run in parallel at the fixed code phase offset. The receiver sequentially performs several tests, each over a period of T seconds, after which a majority decision is made. If out of A tests, there are B tests where the output of the noncoherent correlator exceeds a threshold Ξ_2 set for the verification mode, coarse alignment between the PN codes is assumed and the tracking process follows. If a correct code phase is handed to the code tracking system, the acquisition process is terminated; otherwise, if a false code phase is passed, the acquisition process is reactivated after KT penalty time with a constant K . With the double dwell search, a relatively low threshold Ξ_1 can be used to increase the detection probability, and the verification mode operation can reduce the probability of a false-alarm event; therefore, the mean acquisition time can be greatly reduced.

It has been shown that, in an AWGN channel 1) the decision variables from adjacent correlators are correlated due to MAI, where the local PN subcodes are offset by a phase less than or equal to one chip [10] and 2) successive decision variables from each noncoherent correlator are statistically independent for $\Delta = 1$ or $1/2$ [5] (this argument is applicable to the situation with MAI). Using the hybrid parallel search, in each group of the N_1 simultaneous tests, the code phase offset between the PN subcodes loaded in the adjacent parallel branches is M chips. As a result, the MN_1/Δ decision variables used in each detection are statistically independent in an AWGN channel. In a fading channel, however, there may exist correlation among the decision variables to a certain degree because channel fading status may be correlated over a

number of successive chips. On the other hand, in the case that the parameter Δ is less than one, there exist more than one decision variable with a nonzero ν^2 value corresponding to an " H_1 " cell. In the following, in order to make the performance analysis tractable, the assumptions made in [5]–[8] are adopted here: 1) all the decision variables are independent; and 2) there is only one decision variable corresponding to the correct code phase, i.e., one " H_1 " cell only (neglecting all other possible " H_1 " cells with a smaller nonzero ν^2 value). It is possible that the assumption may result in the theoretical analysis results slightly deviating from practical values, however the general analysis and conclusions (on the effects of search strategies, MAI and noise, and channel fading statistics) given in Section IV should be applicable to a practical system.

In the first dwell (search mode), if the decision variable e of the branch corresponding to the " H_1 " state is larger than all the rest $MN_1/\Delta - 1$ decision variables and, at the same time, is also larger than the threshold Ξ_1 , then the " H_1 " state is sensed correctly. Hence, the probability of detection in the first dwell is

$$P_{d1} = \int_{\Xi_1}^{\infty} f(e|H_1) \left[\int_0^e f(x|H_0) dx \right]^{MN_1/\Delta-1} de \quad (22)$$

Substituting (20) and (21) into (22), it can be obtained that

$$P_{d1} = \sum_{i=0}^{MN_1/\Delta-1} (-1)^i \binom{MN_1}{i} \exp \left[-\frac{i\nu^2}{2(\sigma_0^2 + i\sigma_1^2)} \right] \cdot Q \left(\sqrt{\frac{\sigma_0^2\nu^2}{\sigma_1^2(\sigma_0^2 + i\sigma_1^2)}}, \sqrt{\frac{\sigma_0^2 + i\sigma_1^2}{\sigma_0^2\sigma_1^2}} \Xi_1 \right) \quad (23)$$

where $Q(a, b)$ is the Marcum Q -function defined as

$$Q(a, b) = \int_b^{\infty} x \exp \left(-\frac{x^2 + a^2}{2} \right) I_0(ax) dx.$$

The probability of missing, P_{m1} , in the search mode is the conditional probability that all the MN_1/Δ decision variables are less than Ξ_1 given that one of the decision variable corresponds to the correct code phase, i.e.

$$P_{m1} = \int_0^{\Xi_1} f(e|H_1) \left[\int_0^{\Xi_1} f(x|H_0) dx \right]^{MN_1/\Delta-1} de \quad (24)$$

which can be further derived from (20)–(21) as

$$P_{m1} = \left[1 - \exp \left(-\frac{\Xi_1}{2\sigma_0^2} \right) \right]^{MN_1/\Delta-1} \cdot \left[1 - Q \left(\frac{\nu}{\sigma_1}, \frac{\sqrt{\Xi_1}}{\sigma_1} \right) \right]. \quad (25)$$

The event of a false alarm can occur in two different cases: 1) when the correct code phase is searched but $e_{\max} > \Xi_1$ results from a reference PN code phase corresponding to an " H_0 " state; and 2) when the correct code phase is not searched but e_{\max} is still larger than Ξ_1 . The false-alarm probability corresponding to an " H_1 " state is

$$P_{f11} = 1 - P_{d1} - P_{m1} \quad (26)$$

and corresponding to an “ H_0 ” state is

$$P_{f10} = \frac{MN_1}{\Delta} \int_{\Xi_1}^{\infty} f(e|H_0) \cdot \left[\int_0^e f(x|H_0) dx \right]^{MN_1/\Delta-1} de. \quad (27)$$

Substituting (21), the calculation of P_{f10} can be simplified to

$$P_{f10} = 1 - \left[1 - \exp\left(-\frac{\Xi_1}{2\sigma_0^2}\right) \right]^{MN_1/\Delta}. \quad (28)$$

It is observed that the probabilities (P_{d1} , P_{m1} , P_{f11} , and P_{f10}) depend on the threshold Ξ_1 , the ratio of the received signal power $\gamma_1^2 P$ to noise spectral density N_0 , the normalized synchronization error ϵ_1 , the number of users L in the system, and the channel fading statistics.

The probabilities of detection and false-alarm in the verification mode with a threshold Ξ_2 are

$$P_{d2} = \sum_{i=B}^A \binom{A}{i} p_{d2}^i (1 - p_{d2})^{A-i} \quad (29)$$

and

$$P_{f2} = \sum_{i=B}^A \binom{A}{i} p_{f2}^i (1 - p_{f2})^{A-i} \quad (30)$$

respectively, where

$$\begin{aligned} p_{d2} &= \int_{\Xi_2}^{\infty} f(e|H_1) de \\ &= Q\left(\frac{\nu}{\sigma_1}, \frac{\sqrt{\Xi_2}}{\sigma_1}\right) \end{aligned} \quad (31)$$

and

$$\begin{aligned} p_{f2} &= \int_{\Xi_2}^{\infty} f(e|H_0) de \\ &= \exp\left(-\frac{\Xi_2}{2\sigma_0^2}\right). \end{aligned} \quad (32)$$

The overall probabilities with the double-dwell search are

$$\begin{aligned} P_D &= P_{d1} P_{d2}, \\ P_{F1} &= P_{f11} P_{f2}, \\ P_{F0} &= P_{f10} P_{f2}. \end{aligned} \quad (33)$$

The PN code acquisition can be described as a discrete-time Markov process. Since there exists a duality between the state transition diagram of a discrete-time Markov process and the flow graphs of electrical systems, the flow graph technique has been used to calculate the mean time of PN code acquisition [5]. The acquisition process is modeled as a finite-state Markov process with the transitions among states being determined by the events of detection, false alarm, and missing at each test. The flow graph diagram for the hybrid parallel search is shown in Fig. 3. There are N_2 acquisition states corresponding to the N_2 search intervals for all possible PN code phases. Only acquisition state “1” contains the correct code phase, all the rest $N_2 - 1$ acquisition states correspond to an “ H_0 ” state. With the uniform distribution of the incoming PN code phase over the whole PN code period Θ , each state is tested with a probability of $1/N_2$. Over each interval

T , MN_1/Δ possible incoming code phases are searched once. The transitions shown in Fig. 3 are discussed in the following.

- 1) In acquisition “state 1,” the correct PN code phase is tested. Depending on the decision variables, there are three possible transitions from the state—
 - a) To detection with branch gain $H_{D,I}(z)$: the correct code phase is detected in the first dwell and verified in the second dwell, then the acquisition process is finished.
 - b) To acquisition “state 2” with branch gain $H_M(z)$: this transition happens under three situations, i.e., b-i) if $e_{\max} < \Xi_1$, no coarse alignment is sensed in the first dwell; b-ii) if $e_{\max} > \Xi_1$ occurs where e_{\max} corresponds to an “ H_1 ” state but the first dwell detection is not verified in the second dwell, then the acquisition process is advanced to test the next MN_1/Δ possible incoming code phases; or b-iii) if $e_{\max} > \Xi_1$ occurs where e_{\max} corresponds to an “ H_0 ” state and the false alarm is detected in the second dwell.
 - c) To false alarm with branch gain $H_{F1}(z)$: if in the first dwell $e_{\max} > \Xi_1$ occurs where e_{\max} corresponds to an “ H_0 ” state, and the search is verified in the second dwell, then the acquisition system passes a false code phase to the PN code tracking system, i.e., the acquisition system enters into a false alarm state.
- 2) In acquisition “state i ” ($i = 2, 3, \dots, N_2$), no “ H_1 ” cell is tested, and there are two transitions from the state:
 - a) To acquisition “state $i + 1$ ” if $i < N_2$ and to acquisition “state 1” if $i = N_2$: this happens with branch gain $H_{NF}(z)$ if there is no false alarm.
 - b) To false alarm with branch gain $H_{F0}(z)$: this happens if an incorrect PN code phase is sensed in the first dwell and is also verified in the second dwell.
- 3) From false alarm to acquisition with branch gain $H_R(z)$: once the acquisition system enters a false alarm state, it will take KT penalty time for the system to detect that a false-alarm event has occurred and to re-enter the next acquisition state.

From Fig. 3, the functional transfer function can be derived as shown in (34) (shown at the bottom of the next page) where

$$H_T(z) = H_{NF}(z) + H_{F0}(z)H_R(z) \quad (35)$$

with $H_{NF}(z)$ and $H_{F0}(z)$ being the branch gains corresponding to non false alarm and false alarm transitions, respectively, in an “ H_0 ” state, defined as

$$H_{NF}(z) = (1 - P_{f10})z^T + P_{f10}z^T(1 - P_{f2})z^{AT} \quad (36)$$

$$\begin{aligned} H_{F0}(z) &= P_{f10}z^T P_{f2}z^{AT} \\ &= P_{F0}z^{(A+1)T}. \end{aligned} \quad (37)$$

Other branch gains are

$$\begin{aligned} H_D(z) &= (P_{d1}z^T)(P_{d2}z^{AT}) \\ &= P_D z^{(A+1)T} \end{aligned} \quad (38)$$

$$\begin{aligned} H_{F1}(z) &= (P_{f11}z^T)(P_{f2}z^{AT}) \\ &= P_{F1} z^{(A+1)T} \end{aligned} \quad (39)$$

$$\begin{aligned} H_M(z) &= P_{m1}z^T + P_{d1}z^T(1 - P_{d2})z^{AT} \\ &\quad + P_{f11}z^T(1 - P_{f2})z^{AT} \end{aligned} \quad (40)$$

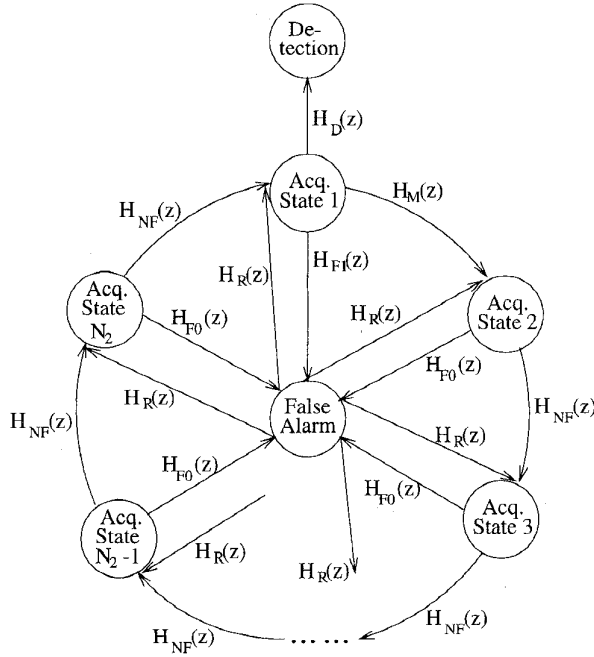


Fig. 3. Flow graph diagram for the hybrid parallel search.

$$H_R(z) = z^{KT}. \quad (41)$$

The mean acquisition time and its variance can be derived as

$$\begin{aligned} E[T_{acq}] &= \left. \frac{dH(z)}{dz} \right|_{z=1} \\ &= \frac{T}{P_D} [1 + A(1 - P_{m1}) + KP_{F1} \\ &\quad + (N_2 - 1)(1 + KP_{F0} + AP_{f10})] \end{aligned} \quad (42)$$

and

$$V[T_{acq}] = \left\{ \frac{d^2H(z)}{dz^2} + \frac{dH(z)}{dz} - \left[\frac{dH(z)}{dz} \right]^2 \right\} \Bigg|_{z=1} \quad (43)$$

When $N_2 = 1$, the hybrid parallel acquisition becomes totally parallel acquisition, and the mean acquisition time is

$$E[T_{acq}] = \frac{T}{P_D} [1 + A(1 - P_{m1}) + KP_{F1}] \quad (44)$$

which is consistent with the result given in [8]. It should be pointed out that in (42) and (44), the mean acquisition time, $E[T_{acq}]$, is not linearly proportional to the correlation time interval, T , because the probabilities (P_D , P_{m1} , P_{F1} , P_{F0} , and P_{f10}) also depend on the value of T . Numerical analysis on the acquisition performance of the hybrid parallel search and totally parallel search is given in (34).

IV. NUMERICAL RESULTS AND DISCUSSION

The above acquisition performance analysis is applied to a system with code period of 32768 chips (using IS-95 standard as a reference [13]). Three integration (correlation) intervals are considered for the noncoherent correlator with $M = 5$ and 1024, respectively. The parameters $\epsilon_1 = 0$ for the “ H_1 ” state and $\Delta = 1/2$ are chosen. The parameter N_2 characterizing the search strategy is selected to be ten for a hybrid parallel search and one for a totally parallel search. The threshold parameters Ξ_1 and Ξ_2 are adjusted to minimize the mean acquisition time in each situation. The parameters of A and B of the verification mode are quoted from [5] to be four and two, respectively. The penalty factor K for the false alarm is selected as two, i.e., the penalty time is $2T$ s. The SNR/chip is defined as the received signal average energy per chip from the intended transmission, including both deterministic component and diffusive component, to one-sided power spectral density N_0 of input noise. The power spectral density of the fading process is given by the classical Doppler spectrum formula, i.e., the autocorrelation functions of the in-phase and quadrature components, $x_i(t)$ and $y_i(t)$, $i = 1, 2, \dots, L$, are [14]

$$\begin{aligned} R_{x_i}(\rho) &= R_{y_i}(\rho) \\ &= \sigma_f^2 J_0(2\pi f_d \rho) \end{aligned} \quad (45)$$

where $J_0(\cdot)$ is zeroth-order Bessel function and f_d is the maximum Doppler frequency shift. This is a more realistic channel model than that adopted in [7] and [8], where the fading process is assumed to be time-invariant over certain successive chips and to be independent from each group of the chips to the others. The channel fading rate normalized to chip rate is 10^{-3} . It is assumed that each transmission has the same average signal power at the receiver and that the k factor of the Rician fading is the same for the target transmission and all other transmission.

A. Effect of Search Strategies

Fig. 4 shows the mean acquisition time in chips as a function of $L - 1$, which is the number of users in the system except the target transmission. The parameters SNR/chip and k are chosen to be -5 and 0 dB, respectively, and the parameter M to be: a) 256, b) 512, and c) 1024. Two search strategies are considered: the totally parallel search with $N_2 = 1$ and the hybrid parallel search with $N_2 = 10$. From Fig. 4, the following are observed.

- 1) The mean acquisition time increases significantly as the MAI (characterized by the number of $L - 1$) increases, no matter which search scheme is used.

$$\begin{aligned} H(z) &= \frac{H_D(z)}{1 - [H_M(z) + H_{F1}(z)H_R(z)][H_T(z)]^{N_2-1}} \sum_{i=1}^{N_2} \frac{1}{N_2} [H_T(z)]^{N_2-i} \\ &= \frac{1}{N_2} \frac{H_D(z) \{1 - [H_T(z)]^{N_2}\}}{\{1 - [H_M(z) + H_{F1}(z)H_R(z)][H_T(z)]^{N_2-1}\} [1 - H_T(z)]}. \end{aligned} \quad (34)$$

- 2) Among the totally parallel searches with three values of M , when there is no MAI (i.e., $L - 1 = 0$), using $M = 256$ gives the best performance; the mean acquisition time increases as the value of M increases. As the MAI increases, the situation changes. Using a larger value of M reduces the mean acquisition time. When $L - 1 \geq 80$, using $M = 1024$ yields the best performance and $M = 256$ the worst. This phenomenon can be explained as follows: In the absence of the MAI, the correlation interval corresponding to $M = 256$ is large enough to achieve a small variance of the decision variables so that code acquisition can be achieved correctly. As a result, using a smaller M value speeds up the acquisition process, i.e., a smaller T value in (44) plays a dominant role in reducing $E[T_{acq}]$. In the presence of the MAI, the SNR value of the decision variables decreases. A longer correlation interval (i.e., a larger M value) is necessary to ensure a high detection probability and a low false-alarm probability and, therefore, to keep a small value of the mean acquisition time. As a result, a larger M value results in better acquisition performance when the MAI is severe. In this case, the increased probability of detection and decreased probabilities of false alarm and missing (resulting from a larger T value) play a dominant role in reducing $E[T_{acq}]$ of (44).
- 3) Comparing the totally parallel search with the hybrid parallel search, when there is no MAI ($L - 1 = 0$), the totally parallel search with any of the M values gives better performance than the hybrid parallel search as expected, which is obtained at the expense of the hardware complexity. However, when the MAI increases to a certain extent ($L > 180$), the hybrid search with $M = 256$ has the better performance than the totally parallel search with $M = 256$. The reason for the hybrid search to have the performance even better than the totally parallel search (with $M = 256$) can be explained as follows. With the totally parallel search, each decision is made based on the decision variables corresponding to all possible PN code phases. Among the Θ/Δ variables, only one corresponds to the correct code phase. Because of the severe MAI, the difference between the pdf's $f(e|H_1)$ and $f(e|H_0)$ is reduced; therefore, the large number of decision variables corresponding to an " H_0 " state makes every possibility for a false alarm event to occur. Using the hybrid search, each decision is made based on $(\Theta/\Delta)/10$ variables. With this much less number of the decision variables corresponding to an " H_0 " state, the false-alarm probability is not increased by the MAI so severely as in the case of using the totally parallel search. The reduced false-alarm probability results in the better acquisition performance of the hybrid search.
- 4) The totally parallel search with $M = 512$ and $M = 1024$ always has better performance than the hybrid search with the same M value when $L - 1 \leq 200$. That is, the totally parallel search outperforms the hybrid search if the parameter M is chosen properly. The optimal value of M increases as the degree of the MAI increases.

However, it is also observed that, as the MAI increases, the advantage of the totally parallel search over the hybrid search on the mean acquisition time is lessened. Taking into account the hardware complexity, the hybrid parallel search is a better choice in the case of severe MAI. For example, using the hybrid search ($N_2 = 10$) with hardware complexity being approximately one-tenth of the totally parallel search ($N_2 = 1$) hardware complexity, the mean acquisition time is increased by 2–3 times when $M = 512$ or 1024 and $L - 1 = 0$ –200. In other words, $E[T_{acq}]$ is increased at a much slower rate than the rate at which the hardware complexity is decreased.

- 5) Similar to the totally parallel search, the hybrid parallel search with a smaller value of M has a shorter mean acquisition time in the case of no MAI; however, it has a longer mean acquisition time in the case of severe MAI. Using the hybrid search scheme, a small value of M means a proportional increase of parallel branches (for $N_2 = 10$), which increases the complexity of the acquisition system on the whole. As a result, using a smaller M value (i.e., a larger number of parallel branches) speeds up the acquisition process at the expense of system complexity.

It should be pointed out that the optimal correlation interval, MT_c , for the minimum mean acquisition time depends on the search strategy, MAI, channel statistics and other system design parameters. Theoretically, the totally parallel search will always outperform the hybrid search if both search schemes use their optimal M values, respectively, as discussed in 4). However, in practice, the optimal value of M for each search changes with time due to the dynamics of channel fading statistics and the time-varying number of users in the system. In the case that the hybrid search has an M value close to its optimal one and the totally parallel search has an M value far away from its optimal one, it is possible that the hybrid search may have better performance than the totally parallel search as discussed in 3).

B. Effect of MAI and Noise

Fig. 5 illustrates the effect of MAI on the acquisition performance with $M = 512$, $k = 0$ dB, and SNR/chip = -25 , -15 , and -5 dB, respectively. The mean acquisition time increases as $L - 1$ increases and/or as SNR/chip decreases in a similar pattern when using: (a) the totally parallel search with $N_2 = 1$ and (b) the hybrid parallel search with $N_2 = 10$. The following are observed.

- 1) The performance improvement achieved by increasing SNR/chip from -25 to -15 dB is much more significant than by increasing SNR/chip from -15 to -5 dB, because a large enough SNR value (larger than a threshold) at the correlator outputs is necessary to ensure a high detection probability and a low false-alarm probability.
- 2) Without MAI (i.e., at $L - 1 = 0$), increasing the SNR/chip value significantly reduces the mean acquisition time. However, with an increase of MAI, the acqui-

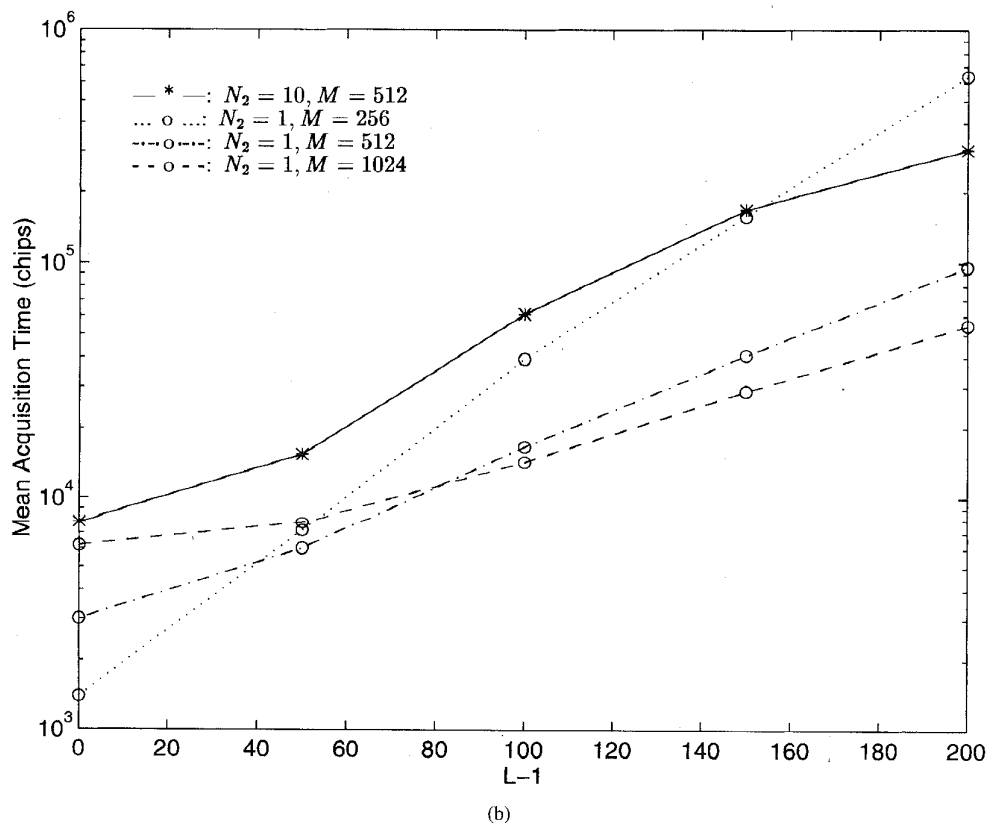
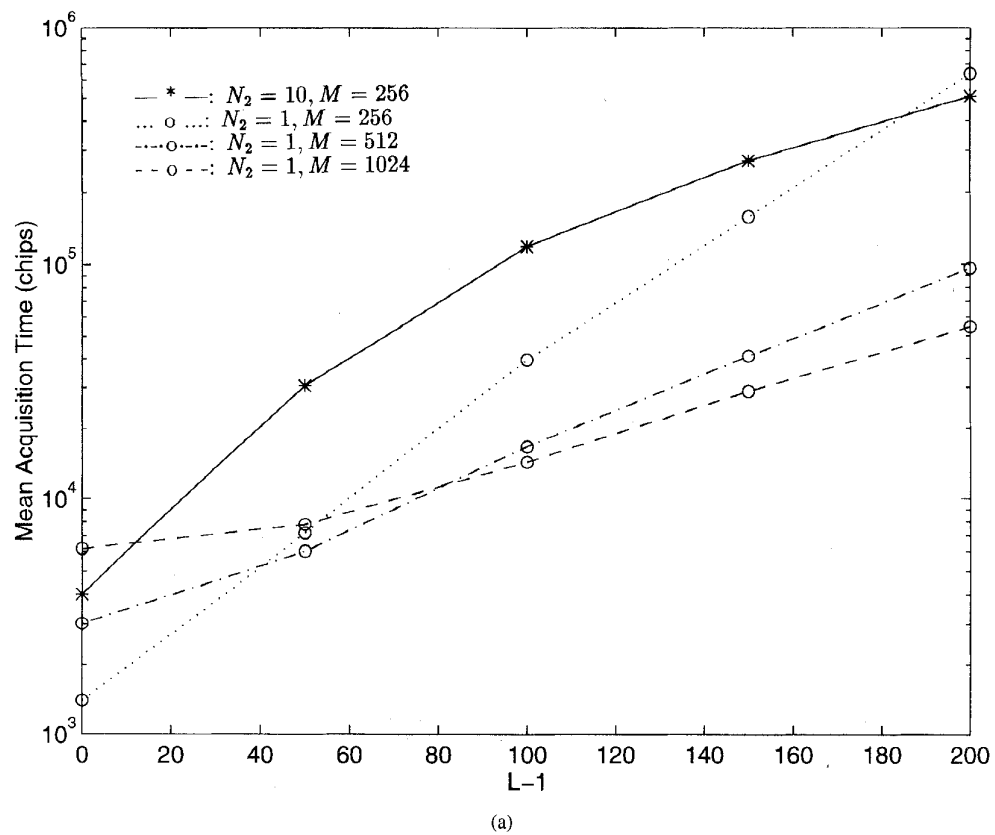


Fig. 4. Mean acquisition time versus $L - 1$, SNR/chip = -5 dB, $k = 0$ dB. (a) $M = 256$, $N_2 = 10$ and $M = 256, 512, 1024$, $N_2 = 1$. (b) $M = 512$, $N_2 = 10$ and $M = 256, 512, 1024$, $N_2 = 1$.

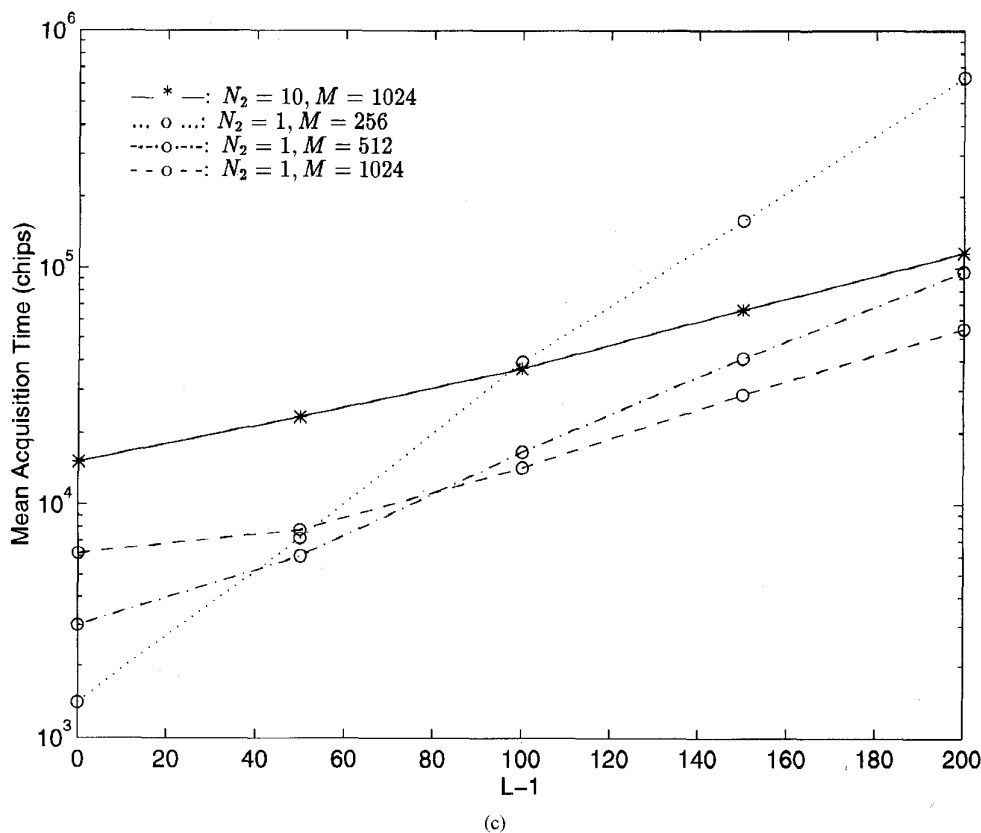


Fig. 4. (Continued) Mean acquisition time versus $L-1$, SNR/chip = -5 dB, $k = 0$ dB. (c) $M = 1024$, $N_2 = 10$ and $M = 256, 512, 1024$, $N_2 = 1$.

sition performance improvement achieved by increasing SNR/chip is reduced. This is because both AWGN and MAI deteriorate the performance. In the case of a small L value, the input white noise is a dominant factor in degrading the acquisition performance, so that the decrease of SNR/chip value significantly increases the mean acquisition time. As the L value increases, a reduction of input noise alone does not improve the performance as significantly as in the case of no MAI.

C. Effect of Channel Fading Statistics

Fig. 6 shows the dependence of the acquisition performance on MAI for various channel fading conditions, with $M = 512$ and SNR/chip = -5 dB, and the k -factor of the Rician channel fading being ∞ dB (AWGN channel), 5 dB, 0 dB, -5 dB and $-\infty$ dB (Rayleigh fading channel), respectively. The following are observed.

- 1) Both channel fading and MAI impair the acquisition performance. For either of the search schemes, with a larger value of the k -factor, the deterministic component of the received signal increases while the diffusive component decreases. Therefore, the degree of channel fading declines and the acquisition performance is improved.
- 2) The effect of the channel fading itself on the mean acquisition time depends on the number of other users in the system. For totally parallel search without MAI, a Rician

fading channel (with $k = 5$ and 0 dB, respectively) results in only slight acquisition performance degradation as compared with an AWGN channel. However, when k value is reduced to -5 dB and further to $-\infty$ dB, the acquisition in the fading channel has much worse performance because the detection probability is greatly reduced and the false alarm probability is significantly increased (due to the severe fading with less or no LOS component). Generally, with small MAI, channel fading is a major reason for the increase of $E[T_{acq}]$; with severe MAI, the effect of channel fading is relatively reduced as MAI becomes a major concern.

- 3) In the case of the hybrid search, channel fading does not severely degrade the acquisition performance in the absence of MAI, because the SNR value of the decision variables is large enough for correct detection with $M = 512$ even for the fading channels. However, as MAI increases, the reduction of the k -factor of the Rician fading channel significantly increases $E[T_{acq}]$, because the SNR value of the decision variables is reduced as the degree of fading and MAI increase simultaneously. When MAI further increases ($L-1 = 200$), the effect of channel fading itself is reduced because of the dominant role of the severe MAI.

In summary, the acquisition performance degradation due to MAI depends on the PN code search scheme, the SNR/chip value of the input signal, the system design parameters (such as M , N_1 , Δ , Θ), and the channel-fading statistics.

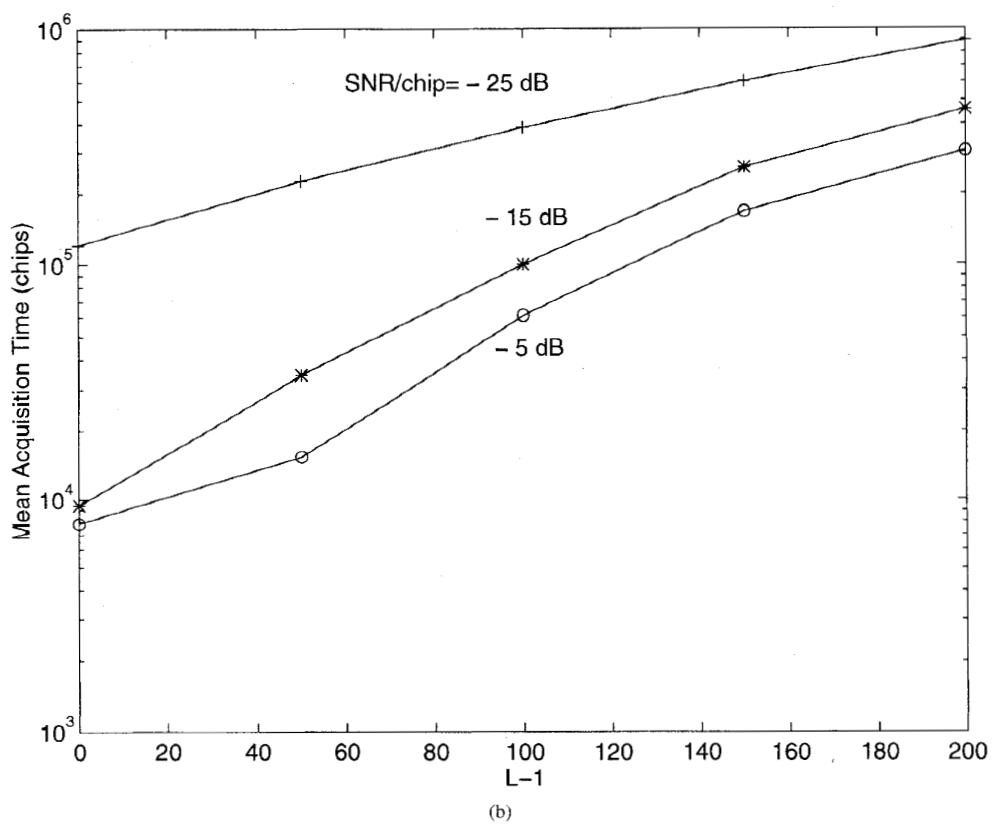
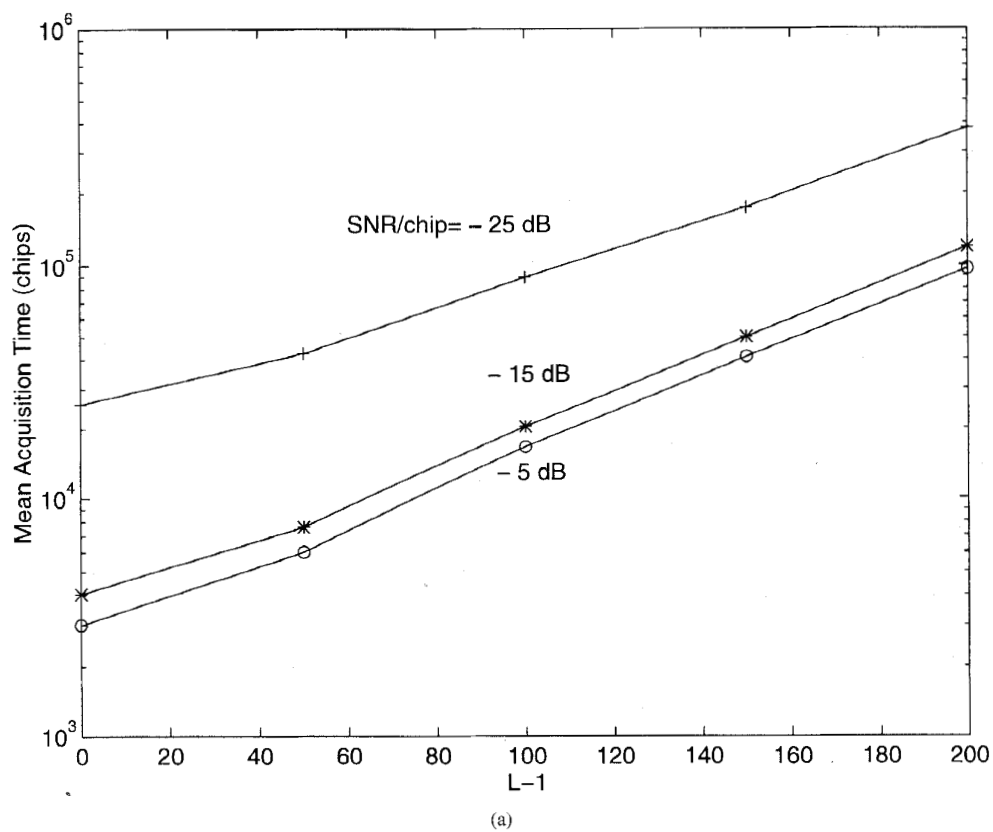


Fig. 5. Mean acquisition time versus $L - 1$, $M = 512$, $k = 0$ dB. (a) Using totally parallel search ($N_2 = 1$). (b) Using hybrid parallel search ($N_2 = 10$).

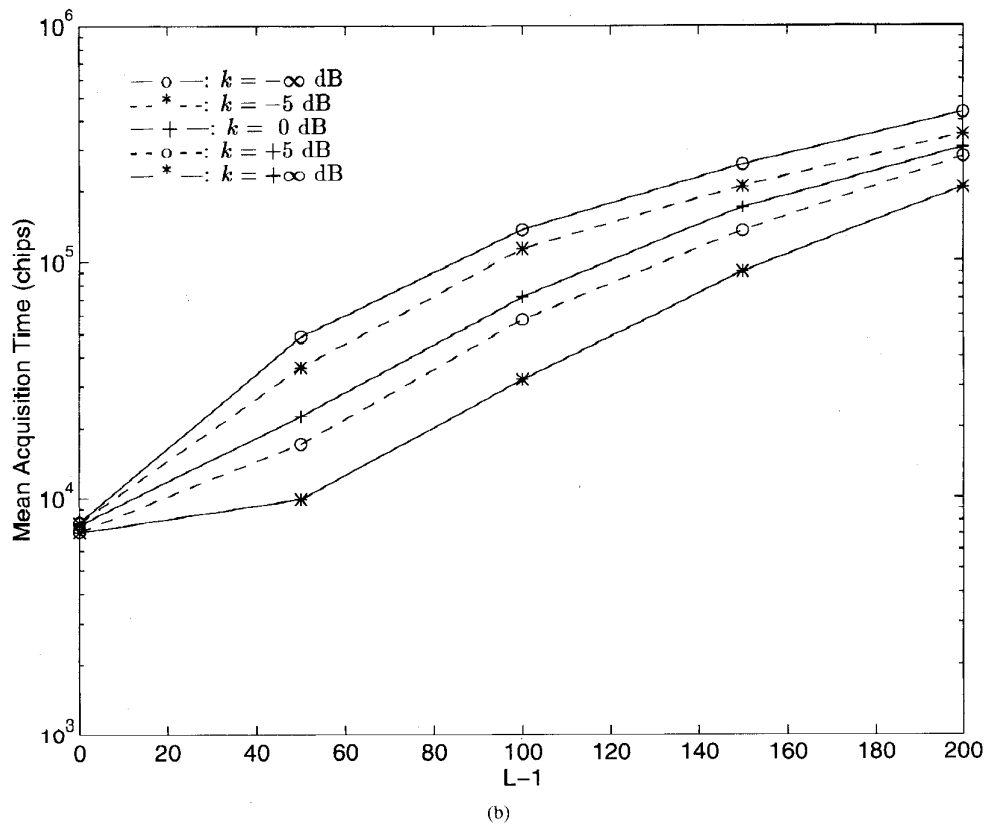
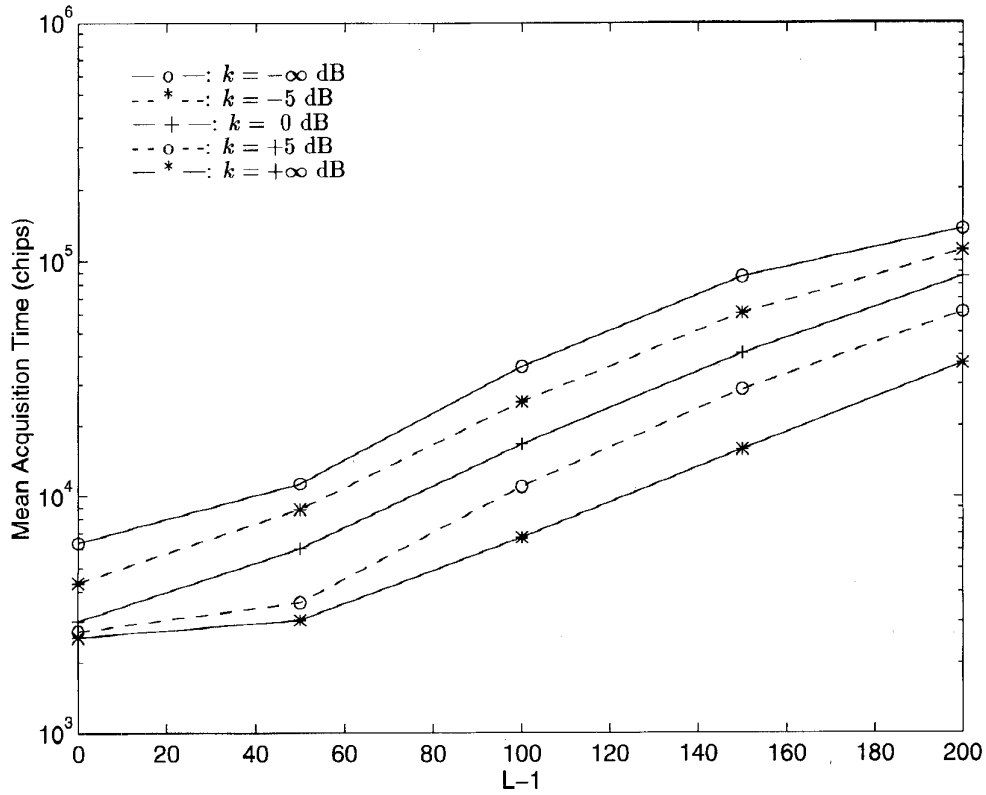


Fig. 6. Mean acquisition time versus $L - 1$, $M = 512$, SNR/chip = 0 dB. (a) Using totally parallel search ($N_2 = 1$). (b) Using hybrid parallel search ($N_2 = 10$).

V. CONCLUSION

The hybrid parallel acquisition scheme has been developed and analyzed for PN code acquisition in the presence of multiple access interference for Rayleigh and Rician fading channels. The proposed hybrid parallel search is of significant importance because it has the much simpler receiver hardware structure compared with the totally parallel search and, at the same time, achieves the acquisition performance much better than that of the totally serial search. Numerical analysis results have quantified the severe acquisition performance degradation of the proposed scheme due to multiple access interference in AWGN, Rayleigh, and Rician fading channels. The increase of the mean acquisition time, due to the interference, depends on the number of users in the system, SNR/chip value of the input signal, system design parameters such as the noncoherent correlation interval (M) and the number of parallel acquisition branches (N_1) and the channel fading statistics.

APPENDIX

In (14)

$$u_i = \frac{1}{T} \int_0^T x_i(t) c_i(t + \xi_i T_c) c_1(t + \hat{\xi}_1 T_c) dt \quad (46)$$

where $x_i(t)$ is a Gaussian random process with zero mean, $c_i(t + \xi_i T_c)$ and $c_1(t + \hat{\xi}_1 T_c)$ take on +1 and -1 values with equal probability. $x_i(t)$, $c_i(t + \xi_i T_c)$ and $c_1(t + \hat{\xi}_1 T_c)$ are mutually independent. As a result, u_i is a Gaussian random variable, with mean

$$\begin{aligned} E[u_i] &= E \left[\frac{1}{T} \int_0^T x_i(t) c_i(t + \xi_i T_c) c_1(t + \hat{\xi}_1 T_c) dt \right] \\ &= \frac{1}{T} \int_0^T E[x_i(t)] E[c_i(t + \xi_i T_c)] E[c_1(t + \hat{\xi}_1 T_c)] dt \\ &= 0. \end{aligned} \quad (47)$$

The variance of u_i is

$$\begin{aligned} \sigma_{u_i}^2 &= E[u_i^2] \\ &= E \left\{ \frac{1}{T^2} \int_0^T \int_0^T [x_i(t) c_i(t + \xi_i T_c) c_1(t + \hat{\xi}_1 T_c)] \right. \\ &\quad \cdot [x_i(s) c_i(s + \xi_i T_c) c_1(s + \hat{\xi}_1 T_c)] dt ds \} \\ &= \frac{1}{T^2} \int_0^T \int_0^T E[x_i(t) x_i(s)] E[c_i(t + \xi_i T_c) c_i(s + \xi_i T_c)] \\ &\quad \cdot E[c_1(t + \hat{\xi}_1 T_c) c_1(s + \hat{\xi}_1 T_c)] dt ds \\ &= \frac{1}{T^2} \int_0^T \int_0^T R_{x_i}(t-s) R_{c_i}(t-s) R_{c_1}(t-s) dt ds \end{aligned} \quad (48)$$

where $R_{x_i}(t-s) = E[x_i(t) x_i(s)]$, $R_{c_i}(t-s) = E[c_i(t) c_i(s)]$, and $R_{c_1}(t-s) = E[c_1(t) c_1(s)]$. Let $\rho = t-s$, then the double integration of (48) can be simplified to a single integration over ρ

$$\sigma_{u_i}^2 = \frac{1}{T^2} \int_{-T}^T R_{x_i}(\rho) R_{c_i}(\rho) R_{c_1}(\rho) (T - |\rho|) d\rho$$

$$\begin{aligned} &= \frac{2}{T^2} \int_0^T (T - \rho) R_{x_i}(\rho) R_{c_i}(\rho) R_{c_1}(\rho) d\rho \\ &= \frac{2}{T^2} \int_0^{T_c} (T - \rho) R_{x_i}(\rho) \left(1 - \frac{\rho}{T_c}\right)^2 d\rho \end{aligned} \quad (49)$$

which is (15).

ACKNOWLEDGMENT

The author is grateful to the anonymous reviewers for their thorough and meticulous reviews, which significantly improve the quality and presentation of this paper.

REFERENCES

- [1] K. S. Gilhousen, I. M. Jacobs, R. Padovani, A. J. Viterbi, A. Weaver, Jr., and C. E. Wheatley, "On capacity of a cellular CDMA system," *IEEE Trans. Veh. Technol.*, vol. 40, pp. 303-312, May 1991.
- [2] W. C. Y. Lee, "Overview of cellular CDMA," *IEEE Trans. Veh. Technol.*, vol. 40, pp. 291-302, May 1991.
- [3] G. L. Stuber and C. Kehao, "Analysis of a multiple-cell direct-sequence CDMA cellular mobile radio system," *IEEE J. Select. Areas Commun.*, vol. SAC-10, pp. 669-679, May 1992.
- [4] L. B. Milstein, T. S. Rappaport, and R. Barghoun, "Performance evaluation for cellular CDMA," *IEEE J. Select. Areas Commun.*, vol. SAC-10, pp. 680-688, May 1992.
- [5] A. Polydoros and C. L. Weber, "A unified approach to serial search spread-spectrum code acquisition—Parts I & II," *IEEE Trans. Commun.*, vol. COM-32, pp. 542-561, May 1984.
- [6] L. B. Milstein, J. Gevorgiz, and P. K. Das, "Rapid acquisition for direct sequence spread-spectrum communications using parallel SAW convolvers," *IEEE Trans. Commun.*, vol. COM-33, pp. 593-600, July 1985.
- [7] E. A. Sourour and S. C. Gupta, "Direct-sequence spread-spectrum parallel acquisition in a fading mobile channel," *IEEE Trans. Commun.*, vol. 38, pp. 992-998, July 1990.
- [8] ———, "Direct-sequence spread-spectrum parallel acquisition in nonselective and frequency-selective Rician fading channels," *IEEE J. Select. Areas Commun.*, vol. 10, pp. 535-544, Apr. 1992.
- [9] U. Madhow and M. B. Pursley, "Acquisition in direct-sequence spread-spectrum communication networks: An asymptotic analysis," *IEEE Trans. Inform. Theory*, vol. 39, pp. 903-912, May 1993.
- [10] R. R. Rick and L. B. Milstein, "Noncoherent parallel acquisition in CDMA spread spectrum systems," in *Proc. ICC'94*, New Orleans, May 1994, pp. 1422-1426.
- [11] R. L. Peterson, R. E. Ziemer, and D. E. Borth, *Introduction to Spread Spectrum Communications*. Englewood Cliffs, NJ: Prentice Hall, 1995, ch. 3 and Appendix D.
- [12] A. Papoulis, *Probability, Random Variables, and Stochastic Processes*, 2nd ed. London: McGraw-Hill, 1984.
- [13] TIA TR45.5 Subcommittee, "An overview of the application of code division multiple access (CDMA) to digital cellular systems and personal cellular networks," May 21, 1992.
- [14] W. C. Jakes, Jr. *Microwave Mobile Communications*. New York: Wiley, 1974.



Weihua Zhuang (M'93) received the B.Sc. (1982) and M.Sc. (1985) degrees from Dalian Marine University (China) and the Ph.D. degree (1993) from the University of New Brunswick (Canada), all in electrical engineering.

Since October 1993, she has been with the Department of Electrical and Computer Engineering, University of Waterloo, Waterloo, Ontario, Canada, where she is an Assistant Professor. Her current research interests include digital transmission over fading channels, wireless networking, and radio positioning. She is a licensed Professional Engineer in the Province of Ontario, Canada.